FRONTIERS OF PHYSICS

RESEARCH ARTICLE
Volume 17 / Issue 6 / 61504 / 2022

The uncertainty and quantum correlation of measurement in double quantum-dot systems

Long-Yu Cheng[1], Fei Ming[1], Fa Zhao[1], Liu Ye[1], Dong Wang[1,2,†]

1 School of Physics and Optoelectronic Engineering, Anhui University, Hefei 230601, China
2 CAS Key Laboratory of Quantum Information, University of Science and Technology of China, Hefei 230026, China
Corresponding author. E-mail: †dwang@ahu.edu.cn
Received February 24, 2022; accepted May 23, 2022

ABSTRACT

In this work, we study the entropic uncertainty and quantum discord in two double-quantum-dot (DQD) system coupled via a transmission line resonator (TLR). Explicitly, the dynamics of the systemic quantum correlation and measured uncertainty are analysed with respect to a general X-type state as the initial state. Interestingly, it is found that the different parameters, including the eigenvalue α of the coherent state, detuning amount δ, frequency ω and the coupling constant g, have subtle effects on the dynamics of the entropic uncertainty, such as the oscillation period of the uncertainty. It is clear to reveal that the quantum discord and the lower bound of the entropic uncertainty are anti-correlated when the initial state of the system is the Werner-type state, while quantum discord and the lower bound of the entropic uncertainty are not anti-correlated when the initial state of the system is the Bell-diagonal state. Thereby, we claim that the current investigation would provide an insight into the entropic uncertainty and quantum correlation in DQDs system, and are basically of importance to quantum precision measurement in practical quantum information processing.

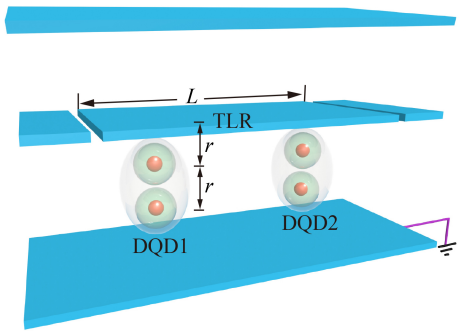

Keywords uncertainty relations, quantum correlation, quantum dot

1 Introduction

The uncertainty principle proposed by Heisenberg is of epoch-making significance to the modern physics, which more clearly distinguishes the difference between the classical and quantum worlds. It has behaved an important feature of quantum mechanics [1]. The uncertainty principle tells us that we cannot determine the quantity of momentum and position at the same time. Kennard [2] firstly formulated the uncertainty principle in the form of standard deviation. Later, Robertson [3] derived an uncertainty relation which is applicable to any pair of noncommutative observables, namely,

$$\Delta\hat{Q}\cdot\Delta\hat{R}\geq\frac{1}{2}|\langle[\hat{Q},\hat{R}]\rangle|, \tag{1}$$

where $\hat{Q}$ and $\hat{R}$ are two non-commutating observables. Note that the lower bound of the relation depends on the state of the system. In order to overcome this shortcoming, Deutsch [4] adopted the form of entropy to describe the uncertainty relation (EUR). Kraus [5], Maassen and Uffink [6] subsequently improved Deutsch's uncertainty relation as follows:

$$H(\hat{Q})+H(\hat{R})\geq-\log_2 c=q_{MU}, \tag{2}$$

where $H(X)=-\sum_i p_i\log_2 p_i$ is the Shannon entropy of the measured observables $X\in(\hat{Q},\hat{R})$ and $p_i=\langle X_i|\rho|X_i\rangle$ is the probability of the outcome i, $c=\max_{ij}|\langle\hat{Q}_i|\hat{R}_j\rangle|^2$ is maximal overlap of $\hat{Q}$ and $\hat{R}$, $|\hat{Q}_i\rangle$ and $|\hat{R}_j\rangle$ correspond to the eigenvectors of $\hat{Q}$ and $\hat{R}$, respectively. Obviously, the lower bound of the inequality is state-independent and

https://doi.org/10.1007/s11467-022-1178-x

related to the measurement selection.

In 2009, Renes and Boileau [7] proposed a new entropic uncertainty relation when there is a quantum memory particle. Later, Berta [8] improved Renes *et al.*'s uncertainty relation with respect to two particles, which can be called the quantum-memory-assisted entropic uncertainty relation (QMA-EUR). Typically, this relation can be explained by a kind of guessing game: there are two participants Alice and Bob, Bob prepares an entangled particle pair (A and B), the particle A is sent to Alice, and the B is used as quantum memory. After Alice receives A, she randomly chooses $\hat{Q}$ or $\hat{R}$ to measure A and attains a measurement result k, and then tells Bob her measurement's choice. In final, Bob's task is to minimize uncertainty to predict Alice's measurement results, relying on the bound of QMA-EUR. Mathematically, this relation can be expressed as [9]

$$S(\hat{Q}|B) + S(\hat{R}|B) \geq -\log_2 c + S(A|B), \tag{3}$$

where $S(\hat{Q}|B) = S(\rho_{\hat{Q}B}) - S(\rho_B)$ represents the conditional von Neumann entropy of post-measurement state with $\rho_{\hat{Q}B} = \sum_i (|\hat{Q}_i\rangle_A\langle\hat{Q}_i| \otimes \mathbb{I}_B)\rho_{AB}(|\hat{Q}_i\rangle_A\langle\hat{Q}_i| \otimes \mathbb{I}_B)$, likewise for $\rho_{\hat{R}B}$. And $S(A|B) = S(\rho_{AB}) - S(\rho_B)$ denotes the conditional von Neumann entropy of systemic density operator $S(\rho_{AB}) = -\mathrm{Tr}(\rho_{AB}\log_2\rho_{AB})$ with $\rho_B = \mathrm{Tr}_A(\rho_{AB})$. According to the QMA-EUR, one can obtain some interesting results as follows: (i) if the conditional von Neumann entropy $S(A|B)$ becomes negative, it means that particles A and B are entangled. When they are at the maximum entanglement, the conditional von Neumann entropy will become $S(A|B) = -\log_2 d$, in this case, the lower bound of the Eq. (3) is zero, in other words, Bob can accurately predict Alice's measurement results. Therefore, whether the conditional von Neumann entropy is negative can be considered as a good criterion of quantum entanglement. (ii) If the memory particle B is not present, Eq. (3) will be reduced to $S(\hat{Q}) + S(\hat{R}) \geq -\log_2 c + S(A)$. Because of $S(A) \geq 0$, this result provides a new lower bound which is tighter than Maassen and Uffink's result. Besides, there are much efforts to contribute to QMA-EUR in theoretical [10– 24] and experimental [25–29] aspects.

Explorations on quantum dots can originate in the 1970s in order to solve the energy crisis. With the continuous in-depth research on quantum dots, there have yielded already many applications, such as lasers [30, 31], light emitting diodes [32, 33], and medicine. Especially, attributing to its relatively long spin coherence time and high controllability, the double quantum dots (DQD) system [35–40] is practically applicable and have been focused widely. On the other hand, the quantum bus function of a transmission line resonator (TLR) [41– 45] has also attracted much attention, and some methods of using TLR to achieve electronically controllable tunnel coupling in quantum dots have been proposed [46–49]. Afterwards, Wu *et al.* [50] explored the dynamic evolution of entanglement correlation and discord correlation when the two DQDs and TLR are prepared in Bell-diagonal and the coherent states. Abdel-Khalek *et al.* [51] studied the relationship between the fidelity, quantum coherence and Bell non-locality when the initial state of this system is the Werner-type state. Noteworthily, there have exhibited some latest efforts on contributing to quantum dots [52– 54]. However, the dynamic evolution of the uncertainty and quantum correlation of the two DQDs system after the measurement has not been studied. Based on this, the aim of this paper is to reveal the dynamic characteristics of the systemic correlation and measurement uncertainty.

The structure of this paper is arranged as follows. In Section 2, we briefly introduce the two DQD-TLR model in detail. In Section 3, we analyze the entropic uncertainty and quantum discord of the system with the different initial states. Finally, a brief summary is given in Section 4.

2 Physical model of DQD-TLR system

In this section, we consider a scenario where the combined system is composed of two DQDs with two electrons and a TLR. In each DQD, two electrons can enter adjacent quantum dots due to tunneling coupling, as shown in Fig. 1. The Hamiltonian of the system can be written as [49, 55–57]

$$\begin{aligned} H_D =& E_S|S_{11}\rangle\langle S_{11}| + (\Delta_0 + E_S)|S_{02}\rangle\langle S_{02}| \\ &+ g_B\mu_B B_e\left(|T_{11}^+\rangle\langle T_{11}^+| - |T_{11}^-\rangle\langle T_{11}^-|\right) \\ &+ E_T|T_{11}^0\rangle\langle T_{11}^0| + t\left(|S_{11}\rangle\langle S_{02}| + |S_{02}\rangle\langle S_{11}|\right), \end{aligned} \tag{4}$$

on the basis of two electrons singlet-triplet states and

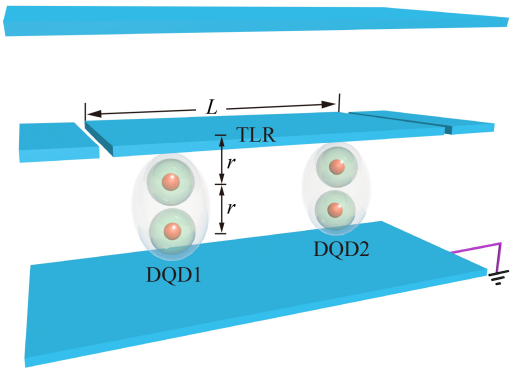

Fig. 1 Schematic of a system consisting of two DQDs and TLR. L denotes the length of the TLR. The two DQDs are labeled as 1 and 2, which positions are located at $L/4$ and $3L/4$ of the TLR respectively, with the external potentials Δ_0^j. The distance between the two quantum dots is r, which is same as that from one of quantum dots to the nearest TLR.

the quantization axis in the z-direction, where

$$|S_{11}\rangle = \frac{1}{\sqrt{2}}\left(|01\rangle - |10\rangle\right), \left|T_{11}^{+}\right\rangle = |00\rangle,$$
$$\left|T_{11}^{0}\right\rangle = \frac{1}{\sqrt{2}}\left(|01\rangle + |10\rangle\right), \left|T_{11}^{-}\right\rangle = |11\rangle$$

are singlet-triplet states of two electron spins in a DQD system. $|S_{02}\rangle$ describes the state in which an electron in a DQD tunneling from one quantum dot to the other, and the two electrons are in a quantum dot at the same time. It should be noted that the subscripts n_u and n_l of these states represent the numbers of electrons in the quantum dot, namely, (n_u, n_l). The role of tunneling t is to couple the $|S_{11}\rangle$ to the $|S_{02}\rangle$. E_S and E_T are the energy of the $|S_{11}\rangle$ and $\left|T_{11}^{0}\right\rangle$ states, respectively. Δ_0 is the energy difference between $|S_{11}\rangle$ and $|S_{02}\rangle$. B_e is the external magnetic field, μ_B is the Bohr magneton and g_B denotes the electron spin g-factor.

Canonically, the Hamiltonian of TLR can be expressed as

$$H_T = \hbar\omega_T\,\phi^{\dagger}\,\phi, \tag{5}$$

where ω_T is the frequency of the TLR, and $\phi^{\dagger}\,(\phi)$ is the creation (annihilation) operator.

Generally, the effective Hamiltonian of the system can be given by [50, 51]

$$\begin{aligned} H_{eff} =& \hbar\omega_T\,\phi^{\dagger}\,\phi + \frac{\hbar}{2}\sum_{j=1}^{2}\left[\omega_j + 2\frac{g^2}{\delta_j}\left(\phi^{\dagger}\,\phi + \frac{1}{2}\right)\right]\sigma_j^z \\ & - \frac{\hbar g^2\left(\delta_1+\delta_2\right)}{2\delta_1\delta_2}\left(\sigma_+^1\sigma_-^2 + \sigma_-^1\sigma_+^2\right), \end{aligned} \tag{6}$$

where the effective coupling constant $g = \frac{g\mu_B\,\mu_0}{8\hbar\pi r}\sqrt{\frac{\hbar\omega_T}{Ll}}$, $\sigma_+^j = |S_{11}\rangle_j\langle T_{11}^0|$ and $\sigma_-^j = \left|T_{11}^0\right\rangle_j\langle S_{11}|$. If the spin qubits are strongly detuned, that is, $|\delta_j| = |\omega_j - \omega_T| \gg g$, $\omega_j = (E_S^j - E_T^j)/\hbar$, and $\sigma_j^z = |S_{11}\rangle_j\langle S_{11}| - \left|T_{11}^0\right\rangle_j\langle T_{11}^0|$. The last term of the above equation describes the commutative state of DQD interacting with TLR.

3 Dynamical characteristics of quantum correlation and measurement uncertainty for DQD-TLR model

In this section, to probe quantum correlation and measurement uncertainty for DQD-TLR model, we have

$$H = \hbar\sum_{j=1}^{2}\Omega_j\,\sigma_j^z - \hbar\chi\left(\sigma_+^1\sigma_-^2 + \sigma_-^1\sigma_+^2\right), \tag{7}$$

when considering the case of DQD interacting with TLR. With the inter-qubit coupling $[\omega_j + 2\frac{g^2}{\delta_j}(\phi^{\dagger}\,\phi + \frac{1}{2})]$, the qubit-TLR coupling $\chi = \frac{g^2(\delta_1+\delta_2)}{2\delta_1\delta_2}$, and the number operator of the TLR is $N = \phi^{\dagger}\,\phi$.

We here label the first and second DQDs as A and B. We first assume that the initial state of this system is X-type state, which can be expressed as

$$\rho\,(0) = \begin{pmatrix} \rho_{11} & 0 & 0 & \rho_{14} \\ 0 & \rho_{22} & \rho_{23} & 0 \\ 0 & \rho_{32} & \rho_{33} & 0 \\ \rho_{41} & 0 & 0 & \rho_{44} \end{pmatrix}. \tag{8}$$

If the initial state of TLR is a coherent state with the form of

$$|\psi_T\,(0)\rangle = |\alpha\rangle_T = \mathrm{e}^{-\frac{1}{2}|\alpha|^2}\sum_{n=0}^{\infty}\frac{\alpha^n}{\sqrt{n!}}|n\rangle, \tag{9}$$

consequently, the reduced density matrix of the system at time t is given as

$$\rho\,(t) = \begin{pmatrix} \rho_{11} & 0 & 0 & \widetilde{\rho}_{14} \\ 0 & \widetilde{\rho}_{22} & \widetilde{\rho}_{23} & 0 \\ 0 & \widetilde{\rho}_{32} & \widetilde{\rho}_{33} & 0 \\ \widetilde{\rho}_{41} & 0 & 0 & \rho_{44} \end{pmatrix}, \tag{10}$$

with

$$\begin{aligned} \tilde{\rho}_{14} =& \rho_{14}\mathrm{e}^{2\mathrm{i}(\omega+g^2/\delta)t}\exp\left[-|\alpha|^2(1-\mathrm{e}^{4\mathrm{i}g^2t/\delta})\right], \\ \tilde{\rho}_{22} =& \frac{1}{2}\left(\rho_{22}+\rho_{33}\right) + \frac{1}{4}\left(\rho_{22}+\rho_{23}-\rho_{32}-\rho_{33}\right)\mathrm{e}^{2\mathrm{i}g^2t/\delta} \\ & + \frac{1}{4}\left(\rho_{22}-\rho_{23}+\rho_{32}-\rho_{33}\right)\mathrm{e}^{-2\mathrm{i}g^2t/\delta}, \\ \tilde{\rho}_{23} =& \frac{1}{2}\left(\rho_{23}+\rho_{32}\right) + \frac{1}{4}\left(\rho_{22}+\rho_{23}-\rho_{32}-\rho_{33}\right)\mathrm{e}^{2\mathrm{i}g^2t/\delta} \\ & + \frac{1}{4}\left(-\rho_{22}+\rho_{23}-\rho_{32}+\rho_{33}\right)\mathrm{e}^{-2\mathrm{i}g^2t/\delta}, \\ \tilde{\rho}_{32} =& \frac{1}{2}\left(\rho_{23}+\rho_{32}\right) + \frac{1}{4}\left(-\rho_{22}-\rho_{23}+\rho_{32}+\rho_{33}\right)\mathrm{e}^{2\mathrm{i}g^2t/\delta} \\ & + \frac{1}{4}\left(\rho_{22}-\rho_{23}+\rho_{32}-\rho_{33}\right)\mathrm{e}^{-2\mathrm{i}g^2t/\delta}, \\ \tilde{\rho}_{33} =& \frac{1}{2}\left(\rho_{22}+\rho_{33}\right) + \frac{1}{4}\left(-\rho_{22}-\rho_{23}+\rho_{32}+\rho_{33}\right)\mathrm{e}^{2\mathrm{i}g^2t/\delta} \\ & + \frac{1}{4}\left(-\rho_{22}+\rho_{23}-\rho_{32}+\rho_{33}\right)\mathrm{e}^{-2\mathrm{i}g^2t/\delta}, \\ \tilde{\rho}_{41} =& \rho_{41}\mathrm{e}^{-2\mathrm{i}\left(\omega+g^2/\delta\right)t}\exp\left[-|\alpha|^2(1-\mathrm{e}^{-4\mathrm{i}g^2t/\delta})\right]. \end{aligned} \tag{11}$$

In what follows, we will discuss the two cases where the initial states of the two DQDs are Werner-type and Bell-diagonal states, respectively.

3.1 Werner-type state

The density matrix of the initial state of the system is the Werner-type state defined by

$$\rho\,(0) = p\,|\beta\rangle\langle\beta| + \frac{1-p}{4}\mathbb{I}_{4\times4}, \tag{12}$$

where $|\beta\rangle = \frac{1}{\sqrt{2}}\left(|00\rangle + |11\rangle\right)$ and $0 \le p \le 1$.

$$\rho_{AB}(t)=\frac{1}{4}\begin{pmatrix}1+p & 0 & 0 & a\\ 0 & 1-p & 0 & 0\\ 0 & 0 & 1-p & 0\\ a^{*} & 0 & 0 & 1+p\end{pmatrix}, \tag{13}$$

with the $a=2p\mathrm{e}^{2\mathrm{i}\left(\omega+g^{2}/\delta\right)t}\exp\left[-|\alpha|^{2}\left(1-\mathrm{e}^{4\mathrm{i}g^{2}t/\delta}\right)\right]$.

Here, by means of two incompatible Pauli operators $\hat{\sigma}_x$ and $\hat{\sigma}_z$, the post-measurement states of subsystem A can be expressed as

$$\begin{aligned}\rho_{xB}&=\sum\nolimits_{i}\left(\left|\hat{\sigma}_{x}^{i}\right\rangle_{A}\left\langle\hat{\sigma}_{x}^{i}\right|\otimes\mathbb{I}_{B}\right)\rho_{AB}\left(\left|\hat{\sigma}_{x}^{i}\right\rangle_{A}\left\langle\hat{\sigma}_{x}^{i}\right|\otimes\mathbb{I}_{B}\right),\\ \rho_{zB}&=\sum\nolimits_{j}\left(\left|\hat{\sigma}_{z}^{j}\right\rangle_{A}\left\langle\hat{\sigma}_{z}^{j}\right|\otimes\mathbb{I}_{B}\right)\rho_{AB}\left(\left|\hat{\sigma}_{z}^{j}\right\rangle_{A}\left\langle\hat{\sigma}_{z}^{j}\right|\otimes\mathbb{I}_{B}\right).\end{aligned} \tag{14}$$

In the above formula, $|\hat{\sigma}_x^i\rangle$ and $|\hat{\sigma}_z^j\rangle$ represent the eigenstates of $\hat{\sigma}_x$ and $\hat{\sigma}_z$, respectively. Therefore, the left-hand side of Eq. (3) will become

$$U_L=S(\rho_{xB})+S(\rho_{zB})-2S(\rho_B), \tag{15}$$

with the von Neumann entropy $S(\rho_{xB})=-\sum_i\lambda_i\log_2\lambda_i$. Meanwhile, we have that the right-hand side of Eq. (3) is equal to

$$U_R=S(\rho_{AB})-S(\rho_B)+1. \tag{16}$$

In order to explore the dynamic characteristics of the uncertainty of the system, we observe the variation curves of the uncertainty U and time t under different parameters which include eigenvalue α of the coherent state, detuning δ, frequency ω and the coupling constant g.

Figure 2 shows the dynamic characteristics of measured uncertainty U in the DQD-TLR model. As shown in Fig. 2(a), one can observe that the oscillation period of U does not change with the growing of the coherent-state eigenvalue α. While, in the same period, the range of the uncertainty reaching peak value is larger with the increasing α. This indicates that the increase of α will induce the inflation of the uncertainty. What's interesting is that, by increasing the parameter δ, one can find in Fig. 2(b) that the oscillation period of U also changes, that is, the larger δ, the smaller oscillation period of U. It is worth noting that in Fig. 2(c), the variation of U is identical with respect to different ω, that is to say, the dynamics of the uncertainty of interest is immune to ω. Different from δ, the oscillation period of U keeps decreasing as g increases as shown in Fig. 2(d). Therefore, we can conclude that, in addition to the frequency ω, changes in the magnitude of the coherent-state eigenvalue α, the detuning δ and the coupling constant g will result in changes in uncertainty.

In order to interpret the nature of the dynamics of the uncertainty, we turn to investigate the evolution of the systemic quantum correlations, which can be quantified by quantum discord (QD). Generally, the quantum discord (QD) is defined as

$$Q(\rho_{AB})=I(A:B)-C(\rho_{AB}), \tag{17}$$

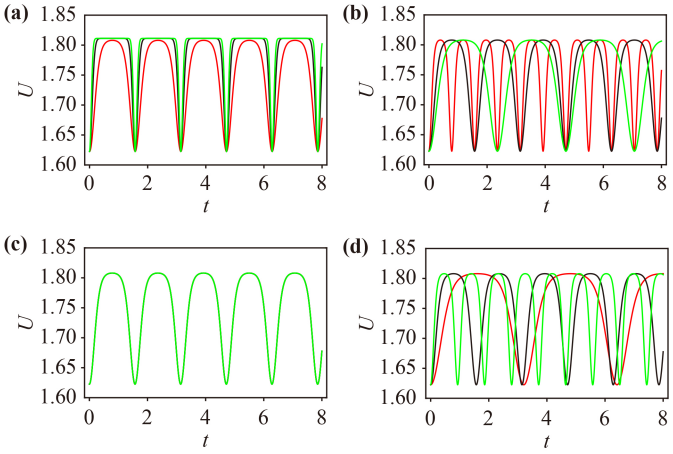

Fig. 2 The entropic uncertainty U with respect to time t in the case of the different eigenvalues α of the coherent state, detuning δ, frequency ω and the coupling constant g. **(a)** $\alpha=1$ (red solid line), $\alpha=2$ (black solid line), $\alpha=3$ (green solid line), with $\omega=1$, $\delta=1$ and $g=1$. **(b)** $\delta=0.5$ (red solid line), $\delta=1$ (black solid line), $\delta=1.5$ (green solid line), with $\omega=1$, $\alpha=1$, $g=1$. **(c)** $\omega=0$ (red solid line), $\omega=2$ (black solid line), $\omega=5$ (green solid line), with $\delta=1$, $\alpha=1$, $g=1$. **(d)** $g=0.7$ (red solid line), $g=1$ (black solid line), $g=1.3$ (green solid line) with $\omega=1$, $\delta=1$, $\alpha=1$. And $p=0.5$ is set for all plotted.

where the mutual information $I(A:B)=S(\rho_A)+S(\rho_B)-S(\rho_{AB})$ indicates the total correlation of the system, and the classical correlation is

$$C(\rho_{AB})=\max_{\left\{\hat{\Pi}_j^A\right\}}\left[S(\rho_A)-S_{\left\{\hat{\Pi}_j^A\right\}}(\rho_{A|B})\right], \tag{18}$$

where $\hat{\Pi}_j^A$ represents the positive operator-valued measure (POVM) acting on subsystem A, and the conditional entropy after the measurement of the subsystem A is $S_{\left\{\hat{\Pi}_j^A\right\}}(\rho_{A|B})=\sum_j p_j S\left(\rho_A^j\right)$. The reduced density matrix after the POVM measurement of subsystem A is $\rho_A^j=\frac{1}{p_j}\mathrm{Tr}_B\left[\left(\hat{\Pi}_j^A\otimes\mathbb{I}^B\right)\rho_{AB}\left(\hat{\Pi}_j^A\otimes\mathbb{I}^B\right)\right]$ with the post-measurement corresponding probability p_j.

Combining Eqs. (3), (17) and (18), the intrinsic relation between the bound of the measured uncertainty and QD can be derived as

$$U_R=\log_2\frac{1}{c}+\min_{\left\{\hat{\Pi}_j^A\right\}}\left[S_{\left\{\hat{\Pi}_j^A\right\}}(\rho_{A|B})\right]-Q(\rho_{AB}). \tag{19}$$

Therefore, we draw the QD and lower bound (U_R) of the entropic uncertainty with respect to t for different parameters, as shown in Fig. 3. Obviously, one can find that U_R and QD exhibit a complete anti-correlation relationship, which is essentially in agreement with the outcome from Eq. (19). Of course, the bound is determined by both QD and the minimal conditional entropy

$\min_{\{\hat{\Pi}_j^A\}}\left[S_{\{\hat{\Pi}_j^A\}}(\rho_{A|B})\right]$, which implies QD and the minimal conditional entropy exist the natural competition. Based on these, we are able to infer that QD plays a leading role in this scenario. More specifically, it is obvious that the oscillation periods of U_R and QD do not change as α increases from Fig. 3(a). In Fig. 3(b), the oscillation periods of U_R and QD increases significantly with the increase of δ, which means that the change of δ has a significant impact on the uncertainty. It is worth noting that ω is insensitive to the variation trend of U_R and QD shown as Fig. 3(c). In sharp contrast to δ, the oscillation periods of U_R and QD decrease with the increase of g in Fig. 3(d).

3.2 Bell-diagonal state

Consider that the initial state of the system is the Bell-diagonal state which is defined as

$$\rho(0)=\frac{1}{4}\left(\mathbb{I}_{AB}+\sum\nolimits_{i=1}^{3}c_i\hat{\sigma}_A^i\otimes\hat{\sigma}_B^i\right), \tag{20}$$

where $c_i\,(0\le|c_i|\le 1)$ are real numbers satisfying the unit trace and positivity conditions of the density operator. When the TLR is prepared in the coherent state, one could derive the final state of the system as

$$\rho_{AB}(t)=\frac{1}{4}\begin{pmatrix}1+c_3 & 0 & 0 & c_0\\ 0 & 1-c_3 & c_1+c_2 & 0\\ 0 & c_1+c_2 & 1-c_3 & 0\\ c_0^* & 0 & 0 & 1+c_3\end{pmatrix}, \tag{21}$$

where $c_0=(c_1-c_2)\,\mathrm{e}^{2\mathrm{i}\left(\omega+g^2/\delta\right)t}\exp\left[-|\alpha|^2\left(1-\mathrm{e}^{4\mathrm{i}g^2t/\delta}\right)\right]$.

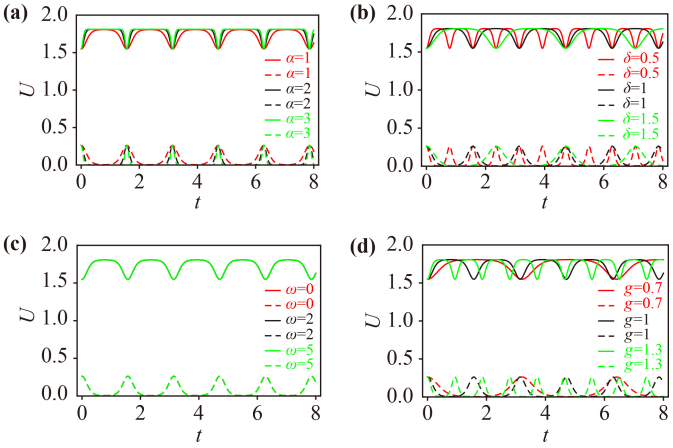

Fig. 3 The lower bound (U_R) of the entropic uncertainty and quantum discord (QD) as a function of time t. The solid lines represent U_R, and the dashed lines represent QD. **(a)** U_R and QD vs. time t for $\omega=1$, $\delta=1$ and $g=1$. **(b)** U_R and QD vs. time t for $\omega=1$, $\alpha=1$ and $g=1$. **(c)** U_R and QD vs. time t for $\delta=1$, $\alpha=1$ and $g=1$. **(d)** U_R and QD vs. time t for $\omega=1$, $\delta=1$ and $\alpha=1$. All results are plotted with $p=0.5$.

After similar calculation processing, the time evolution of the entropic uncertainty and QD in this system has been shown in Fig. 4 and Fig. 5, respectively.

As shown in Fig. 4(a), with the increase of α, the oscillation period of the entropic uncertainty U obviously decreases, and when α is smaller, the oscillation of U becomes more chaotic. Different from α, as plotted in Fig. 4(b), the larger δ is, the oscillation period of U increases. Interestingly, in Fig. 4(c), the oscillation period of time evolution of the entropic uncertainty does not change with the increase of ω. What is more interesting is that the change curves of U in 4(d) are consistent with that in 4(a), that is to say, in this case, the influences of α and g on U are roughly same.

Figure 5 depicts the time evolution of U_R and QD with respect to t. Interestingly, U_R does not show a completely anti-correlation relationship with QD, this is due to minimal conditional entropy $\min_{\{\hat{\Pi}_j^A\}}\left[S_{\{\hat{\Pi}_j^A\}}(\rho_{A|B})\right]$ jointly determine the bound, which means that there is competition between them in nature. Based on these, we can infer that minimal conditional entropy $\min_{\{\hat{\Pi}_j^A\}}\left[S_{\{\hat{\Pi}_j^A\}}(\rho_{A|B})\right]$ plays a leading role in this scenario. As shown in Fig. 5(a), the oscillation period of U_R is identical to QD, and the varying α does not change their periods. For Fig. 5(b), the evolution of U_R and QD with respect to time t both exhibit periodic changes, with the increase of δ, the oscillation periods of the both will become larger, while their periods are not the same. As shown in Fig. 5(c), the change of ω is

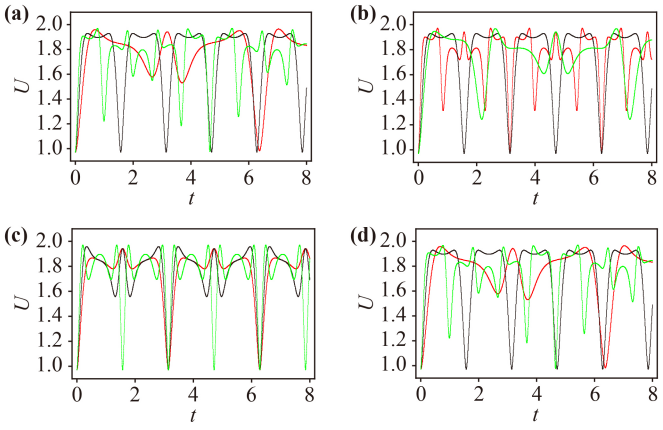

Fig. 4 The entropic uncertainty U with respect to time t in the case of the different eigenvalues α of the coherent state, detuning δ, frequency ω and the coupling constant g. **(a)** $\alpha=1$ (red solid line), $\alpha=2$ (black solid line), $\alpha=3$ (green solid line), with $\omega=1$, $\delta=1$ and $g=1$. **(b)** $\delta=0.5$ (red solid line), $\delta=1$ (black solid line), $\delta=1.5$ (green solid line), with $\omega=1$, $\alpha=1$, $g=1$. **(c)** $\omega=0$ (red solid line), $\omega=2$ (black solid line), $\omega=5$ (green solid line), with $\delta=1$, $\alpha=1$, $g=1$. **(d)** $g=0.7$ (red solid line), $g=1$ (black solid line), $g=1.3$ (green solid line), with $\omega=1$, $\delta=1$, $\alpha=1$. $p=0.5$ is set for all plotted.

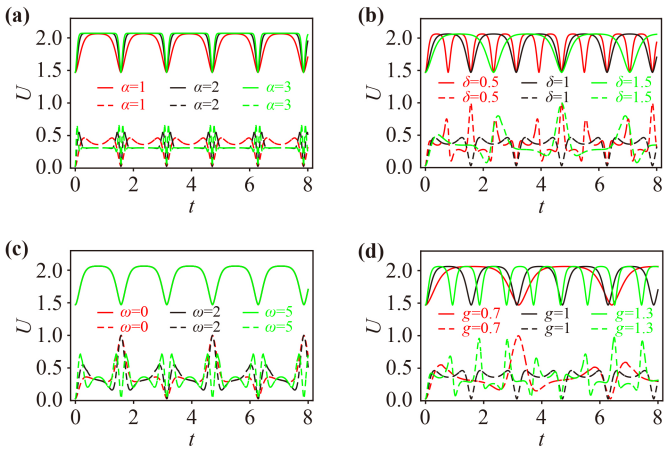

Fig. 5 The lower bound (U_R) of the entropic uncertainty and quantum discord (QD) as a function of time t. The solid lines represent U_R, and the dashed lines represent QD. **(a)** U_R and QD vs. time t for $\omega = 1$, $\delta = 1$ and $g = 1$. **(b)** U_R and QD vs. time t for $\omega = 1$, $\alpha = 1$ and $g = 1$. **(c)** U_R and QD vs. time t for $\delta = 1$, $\alpha = 1$ and $g = 1$. **(d)** U_R and QD vs. time t for $\omega = 1$, $\delta = 1$ and $\alpha = 1$. All results are plotted with $p = 0.5$.

insensitive to the time evolution of U_R and own a slight influence on the variation trend of QD. The oscillation period of QD does not change with the variation of ω. Different from δ, the increase of g leads to the decrease the oscillation periods of U_R and QD.

4 Conclusions and remarks

In this work, we have examined the entropic uncertainty and quantum discord of DQD-TLR system in the case that the initial states are Werner-type state and Bell-diagonal state, respectively. Comparing the dynamics, it has been found that the dynamic evolution of the latter is more complicated. When the initial state of the system is the Werner-type state, different parameters will exhibit different effects on the time evolution of the entropic uncertainty. The lower bound of the entropic uncertainty and quantum discord innately are characterized by anti-correlation relationship, because QD plays a prominent role in determining the bound. With regard to the case of the Bell-diagonal state as the initial state of the system, it is interesting that the lower bound of entropic uncertainty and quantum discord do not show an anti-correlation relationship, this may be because that the minimal conditional entropy becomes a dominant role in determining the magnitude of the uncertainty. To sum up, the current observation offers insight into the dynamics of the quantum correlation and the measured uncertainty in DQD systems, and would be of fundamental importance to perspective quantum information processing in quantum-dot-based frameworks.

Acknowledgements This work was supported by the National Natural Science Foundation of China under Grant Nos. 12075001, 61601002 and 12175001, Anhui Provincial Key Research and Development Plan (Grant No. 2022b13020004), Anhui Provincial Natural Science Foundation (Grant No. 1508085QF139), University Innovation Fund of the Ministry of Education (Grant No. 2021BCA02003), and the fund from CAS Key Laboratory of Quantum Information (Grant No. KQI201701).

References

1. W. Heisenberg, Über den anschaulichen Inhalt der quantentheoretischen Kinematik und Mechanik, *Z. Phys.* 43(3–4), 172 (1927)
2. E. H. Kennard, Zur Quantenmechanik einfacher Bewegungstypen, *Z. Phys.* 44(4–5), 326 (1927)
3. H. P. Robertson, The uncertainty principle, *Phys. Rev.* 34(1), 163 (1929)
4. D. Deutsch, Uncertainty in quantum measurements, *Phys. Rev. Lett.* 50(9), 631 (1983)
5. K. Kraus, Complementary observables and uncertainty relations, *Phys. Rev. D* 35(10), 3070 (1987)
6. H. Maassen and J. B. M. Uffink, Generalized entropic uncertainty relations, *Phys. Rev. Lett.* 60(12), 1103 (1988)
7. J. M. Renes and J.-C. Boileau, Conjectured strong complementary information tradeoff, *Phys. Rev. Lett.* 103(2), 020402 (2009)
8. M. Berta, M. Christandl, R. Colbeck, J. M. Renes, and R. Renner, The uncertainty principle in the presence of quantum memory, *Nat. Phys.* 6(9), 659 (2010)
9. L. J. Li, F. Ming, X. K. Song, L. Ye, and D. Wang, Review on entropic uncertainty relations, *Acta Physica Sinica* 71(7), 070302 (2022)
10. T. Pramanik, S. Mal, and A. S. Majumdar, Lower bound of quantum uncertainty from extractable classical information, *Quantum Inform. Process.* 15(2), 981 (2016)
11. M. L. Hu and H. Fan, Competition between quantum correlations in the quantum-memory-assisted entropic uncertainty relation, *Phys. Rev. A* 87(2), 022314 (2013)
12. P. J. Coles and M. Piani, Improved entropic uncertainty relations and information exclusion relations, *Phys. Rev. A* 89(2), 022112 (2014)
13. S. Liu, L. Z. Mu, and H. Fan, Entropic uncertainty relations for multiple measurements, *Phys. Rev. A* 91(4), 042133 (2015)
14. F. Adabi, S. Salimi, and S. Haseli, Tightening the entropic uncertainty bound in the presence of quantum memory, *Phys. Rev. A* 93(6), 062123 (2016)
15. J. L. Huang, W. C. Gan, Y. L. Xiao, F. W. Shu, and M. H. Yung, Holevo bound of entropic uncertainty in Schwarzschild spacetime, *Eur. Phys. J. C* 78(7), 545 (2018)
16. Y. Y. Yang, W. Y. Sun, W. N. Shi, F. Ming, D. Wang, and L. Ye, Dynamical characteristic of measurement uncertainty under Heisenberg spin models with Dzyaloshinskii–Moriya interactions, *Front. Phys.* 14(3), 31601 (2019)
17. M. N. Chen, D. Wang, and L. Ye, Characterization of

dynamical measurement's uncertainty in a two-qubit system coupled with bosonic reservoirs, *Phys. Lett. A* 383(10), 977 (2019)
18. D. Wang, F. Ming, M. L. Hu, and L. Ye, Quantum-memory-assisted entropic uncertainty relations, *Ann. Phys.* 531(10), 1900124 (2019)
19. F. Ming, D. Wang, X. G. Fan, W. N. Shi, L. Ye, and J. L. Chen, Improved tripartite uncertainty relation with quantum memory, *Phys. Rev. A* 102(1), 012206 (2020)
20. D. Wang, F. Ming, X. K. Song, L. Ye, and J. L. Chen, Entropic uncertainty relation in neutrino oscillations, *Eur. Phys. J. C* 80(8), 800 (2020)
21. H. Dolatkhah, S. Haseli, S. Salimi, and A. S. Khorashad, Tightening the tripartite quantum-memory-assisted entropic uncertainty relation, *Phys. Rev. A* 102(5), 052227 (2020)
22. B. F. Xie, F. Ming, D. Wang, L. Ye, and J. L. Chen, Optimized entropic uncertainty relations for multiple measurements, *Phys. Rev. A* 104(6), 062204 (2021)
23. R. A. Abdelghany, A. B. A. Mohamed, M. Tammam, W. Kuo, and H. Eleuch, Tripartite entropic uncertainty relation under phase decoherence, *Sci. Rep.* 11(1), 11830 (2021)
24. S. Haddadi, M. Ghominejad, A. Akhound, and M. R. Pourkarimi, Suppressing measurement uncertainty in an inhomogeneous spin star system, *Sci. Rep.* 11(1), 22691 (2021)
25. W. C. Ma, Z. H. Ma, H. Y. Wang, Z. H. Chen, Y. Liu, F. Kong, Z. K. Li, X. H. Peng, M. J. Shi, F. Z. Shi, S. M. Fei, and J. F. Du, Experimental test of Heisenbergs measurement uncertainty relation based on statistical distances, *Phys. Rev. Lett.* 116(16), 160405 (2016)
26. Z. X. Chen, J. L. Li, Q. C. Song, H. Wang, S. M. Zangi, and C. F. Qiao, Experimental investigation of multi-observable uncertainty relations, *Phys. Rev. A* 96(6), 062123 (2017)
27. W. M. Lv, C. Zhang, X. M. Hu, H. Cao, J. Wang, Y. F. Huang, B. H. Liu, C. F. Li, and G. C. Guo, Experimental test of the trade-off relation for quantum coherence, *Phys. Rev. A* 98(6), 062337 (2018)
28. H. Y. Wang, Z. H. Ma, S. J. Wu, W. Q. Zheng, Z. Cao, Z. H. Chen, Z. K. Li, S. M. Fei, X. H. Peng, V. Vedral, and J. F. Du, Uncertainty equality with quantum memory and its experimental verification, *npj Quantum Inform.* 5(1), 39 (2019)
29. W. M. Lv, C. Zhang, X. M. Hu, Y. F. Huang, H. Cao, J. Wang, Z. B. Hou, B. H. Liu, C. F. Li, and G. C. Guo, Experimental test of fine-grained entropic uncertainty relation in the presence of quantum memory, *Sci. Rep.* 9(1), 8748 (2019)
30. J. A. Lott, N. N. Ledentsov, V. M. Ustinov, A. Y. Egorov, A. E. Zhukov, P. S. Kopev, Z. Alferov, and D. Bimberg, Vertical cavity lasers based on vertically coupled quantum dots, *Electron. Lett.* 33(13), 1150 (1997)
31. D. L. Huffaker, G. Park, Z. Zou, O. B. Shchekin, and D. G. Deppe, 1.3 m room-temperature GaAs-based quantum-dot laser, *Appl. Phys. Lett.* 73(18), 2564 (1998)
32. H. S. Jang, H. Yang, S. W. Kim, J. Y. Han, S. G. Lee, and D. Y. Jeon, White light-emitting diodes with excellent color rendering based on organically capped CdSe quantum dots and Sr_3SiO_5:Ce^{3+}, Li^+ phosphors, *Adv. Mater.* 20(14), 2696 (2008)
33. Q. Sun, Y. A. Wang, L. S. Li, D. Wang, T. Zhu, J. Xu, and Y. Li, Bright, multicoloured light-emitting diodes based on quantum dots, *Nat. Photonics* 1(12), 717 (2007)
34. V. Bagalkot, L. Zhang, E. Levy-Nissenbaum, S. Jon, P. W. Kantoff, R. Langer, and O. C. Farokhzad, Quantum dot–Aptamer conjugates for synchronous cancer imaging, therapy, and sensing of drug delivery based on bi-fluorescence resonance energy transfer, *Nano Lett.* 7(10), 3065 (2007)
35. V. N. Golovach, A. Khaetskii, and D. Loss, Phonon-induced decay of the electron spin in quantum dots, *Phys. Rev. Lett.* 93(1), 016601 (2004)
36. F. H. L. Koppens, C. Buizert, K. J. Tielrooij, I. T. Vink, K. C. Nowack, T. Meunier, L. P. Kouwenhoven, and L. M. K. Vandersypen, Driven coherent oscillations of a single electron spin in a quantum dot, *Nature* 442(7104), 766 (2006)
37. K. C. Nowack, F. H. L. Koppens, Y. V. Nazarov, and L. M. K. Vandersypen, Coherent control of a single electron spin with electric fields, *Science* 318(5855), 1430 (2007)
38. V. N. Golovach, M. Borhani, and D. Loss, Electric-dipole induced spin resonance in quantum dots, *Phys. Rev. B* 74(16), 165319 (2006)
39. J. R. Petta, A. C. Johnson, J. M. Taylor, E. A. Laird, A. Yacoby, M. D. Lukin, C. M. Marcus, M. P. Hanson, and A. C. Gossard, Coherent manipulation of coupled electron spins in semiconductor quantum dots, *Science* 309(5744), 2180 (2005)
40. T. H. Oosterkamp, T. Fujisawa, W. G. van der Wiel, K. Ishibashi, R. V. Hijman, S. Tarucha, and L. P. Kouwenhoven, Microwave spectroscopy of a quantum-dot molecule, *Nature* 395(6705), 873 (1998)
41. A. Blais, J. Gambetta, A. Wallraff, D. I. Schuster, S. M. Girvin, M. H. Devoret, and R. J. Schoelkopf, Quantum-information processing with circuit quantum electrodynamics, *Phys. Rev. A* 75(3), 032329 (2007)
42. A. Wallraff, D. I. Schuster, A. Blais, L. Frunzio, R. S. Huang, J. Majer, S. Kumar, S. M. Girvin, and R. J. Schoelkopf, Strong coupling of a single photon to a superconducting qubit using circuit quantum electrodynamics, *Nature* 431(7005), 162 (2004)
43. D. I. Schuster, A. A. Houck, J. A. Schreier, A. Wallraff, J. M. Gambetta, A. Blais, L. Frunzio, J. Majer, B. Johnson, M. H. Devoret, S. M. Girvin, and R. J. Schoelkopf, Resolving photon number states in a superconducting circuit, *Nature* 445(7127), 515 (2007)
44. Q. Q. Wu, J. Q. Liao, and L. M. Kuang, Quantum state transfer between charge and flux qubits in circuit-QED, *Chin. Phys. Lett.* 25(4), 1179 (2008)
45. M. A. Sillanpää, J. I. Park, and R. W. Simmonds, Coherent quantum state storage and transfer between two phase qubits via a resonant cavity, *Nature* 449(7161), 438 (2007)
46. Z. R. Lin, G. P. Guo, T. Tu, F. Y. Zhu, and G. C. Guo, Erratum: Generation of quantum-dot cluster states with a superconducting transmission line resonator, *Phys. Rev. Lett.* 101(23), 230501 (2008)
47. P. Pei, C. Li, J. S. Jin, and H. S. Song, Quantum coherence

versus quantum discord in two coupled semiconductor double-dot molecules via a transmission line resonator, *J. Phys. B: At. Mol. Opt. Phys.* 44(3), 035501 (2011)
48. G. Burkard and A. Imamoglu, Ultra-long distance interaction between spin qubits, *Phys. Rev. B* 74(4), 041307 (2006)
49. J. M. Taylor, and M. D. Lukin, Cavity quantum electrodynamics with semiconductor double-dot molecules on a chip, arXiv: cond-mat/0605144 (2006)
50. Q. Q. Wu, Q. S. Tan, and L. M. Kuang, Controllable coupling and quantum correlation dynamics of two double quantum dots coupled via a transmission line resonator, *Eur. Phys. J. B* 83(4), 465 (2011)
51. S. Abdel-Khalek, K. Berrada, and A. Alkaoud, Nonlocality and coherence in double quantum dot systems, *Physica E* 130(23), 114679 (2021)
52. L. X. Liang, Y. Y. Zheng, Y. X. Zhang, and M. Zhang, Error-detected *N*-photon cluster state generation based on the controlledphase gate using a quantum dot in an optical microcavity, *Front. Phys.* 15(2), 21601 (2020)
53. X. Wu and P. Z. Zhao, Nonadiabatic geometric quantum computation protected by dynamical decoupling via the *XXZ* Hamiltonian, *Front. Phys.* 17(3), 31502 (2022)
54. S. Y. Li and L. He, Recent progresses of quantum confinement in graphene quantum dots, *Front. Phys.* 17(3), 33201 (2022)
55. J. M. Taylor, J. R. Petta, A. C. Johnson, A. Yacoby, C. M. Marcus, and M. D. Lukin, Relaxation, dephasing, and quantum control of electron spins in double quantum dots, *Phys. Rev. B* 76(3), 035315 (2007)
56. O. N. Jouravlev and Y. V. Nazarov, Electron transport in a double quantum dot governed by a nuclear magnetic field, *Phys. Rev. Lett.* 96(17), 176804 (2006)
57. F. H. L. Koppens, C. Buizert, I. T. Vink, K. C. Nowack, T. Meunier, L. P. Kouwenhoven, and L. M. K. Vandersypen, Detection of single electron spin resonance in a double quantum dot, *J. Appl. Phys.* 101(8), 081706 (2007)